

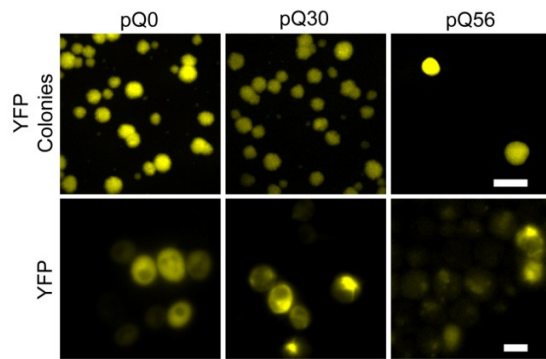
A network of genes connects polyglutamine toxicity to ploidy control in yeast

Christoph J. O. Kaiser¹, Stefan W. Grötzinger¹, Julia M. Eckl¹, Katharina Papsdorf¹, Stefan Jordan² and Klaus Richter¹

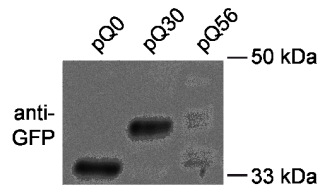
Supplementary Information

Supplementary Figures S1-S13

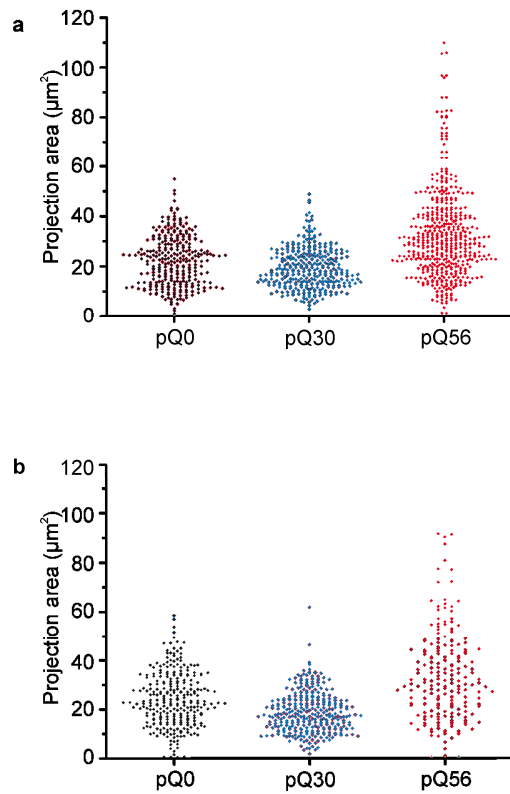
Supplementary Tables S1-S3



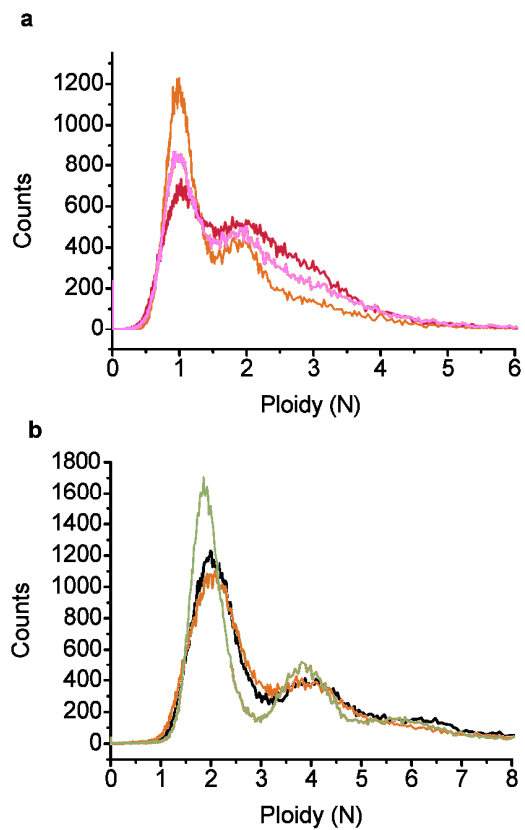
Supplementary Figure S1: Fluorescence properties of pQ0, pQ30 and pQ56 transformed yeast. All colonies of pQ0 and pQ30 transformants show similar fluorescence levels and similar sizes. Fluorescence of small colonies on pQ56-transformed plates is very weak and only a few large colonies show high fluorescence intensities. The scale bar represents 1 mm (upper row). Fluorescence micrographs of yeast cells reveal a homogeneous fluorescence distribution for Q₀-YFP. Q₃₀-YFP in contrast exhibits focal aggregates or fibrous structures. Q₅₆-YFP fluorescence is generally much lower and cells rarely exhibit punctate or focal aggregates. The scale bar represents 5 μ m (lower row).



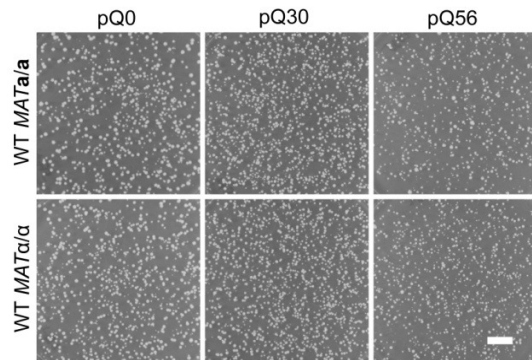
Supplementary Figure S2: Analysis of polyQ expression in WT yeast. Western blotting against YFP using an anti-GFP antibody exhibits distinct protein bands of the correct molecular weight for all three constructs as well as degradation products of Q₅₆-YFP. For pQ0 and pQ30, lysates were diluted 15-fold in comparison to pQ56 to enable simultaneous detection on a single blot.



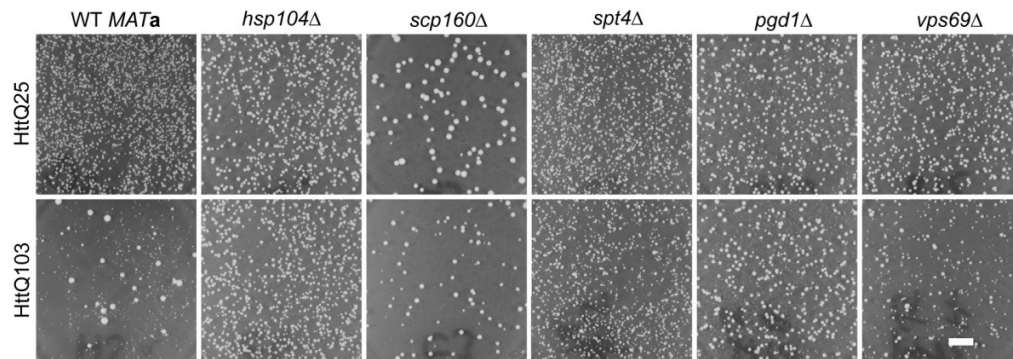
Supplementary Figure S3: Reproducibility of size analysis. To evaluate the reproducibility of the bee-swarm plots presented in Fig. 1 b, two additional biological replicates were subjected to the same assay to estimate cellular size. Both plots are derived from a mixture of small colonies, obtained from two separate inoculates on different days. Evaluated cells were (a) $n=300$, $n=325$ and $n=499$ and (b) $n=279$, $n=316$ and $n=201$ for pQ0, pQ30 and pQ56 transformants, respectively.



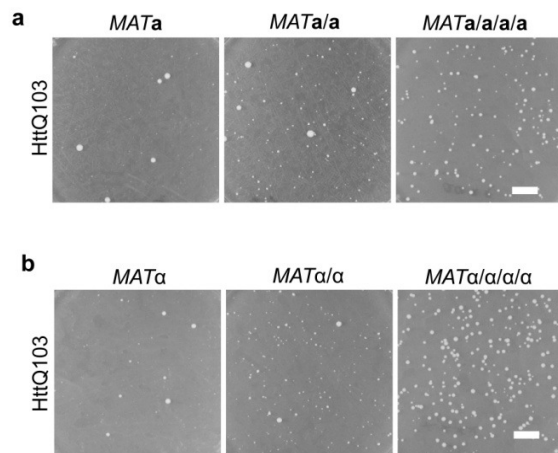
Supplementary Figure S4: FACS analysis of large survivor colonies from pQ56 yeast. (a) Strongly fluorescent large colonies were picked from plates of WT *MATa* yeast transformed with pQ56 and subjected to FACS analysis. Histograms of three representative samples are shown. All samples exhibit mainly a haploid growth pattern. **(b)** Weakly fluorescent large colonies were picked and subjected to the same analysis. Three representative histograms are shown, exhibiting a $\geq 2N/4N$ cycling behavior.



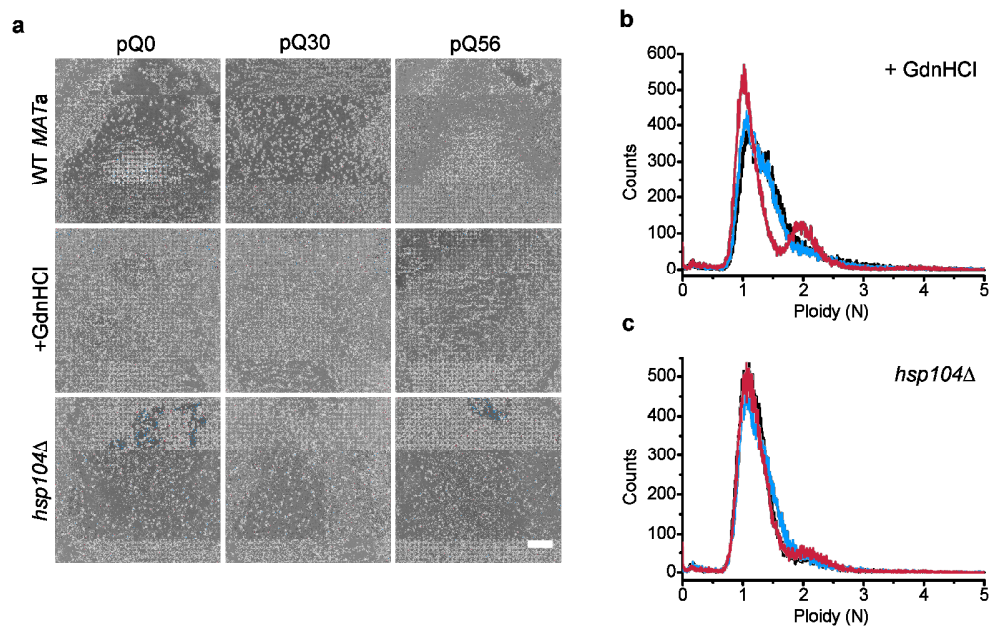
Supplementary Figure S5: *MATa/a* and *MATa/a* yeast are resistant to *pica*. Colony patterns are homogenous after transformation with pQ56 for the yeast strains PY4995 (*MATa/a*, upper row) and PY4994 (*MATa/a*, lower row) indicating that no *pica* phenotype is apparent for these two strains. The scale bar represents 10 mm.



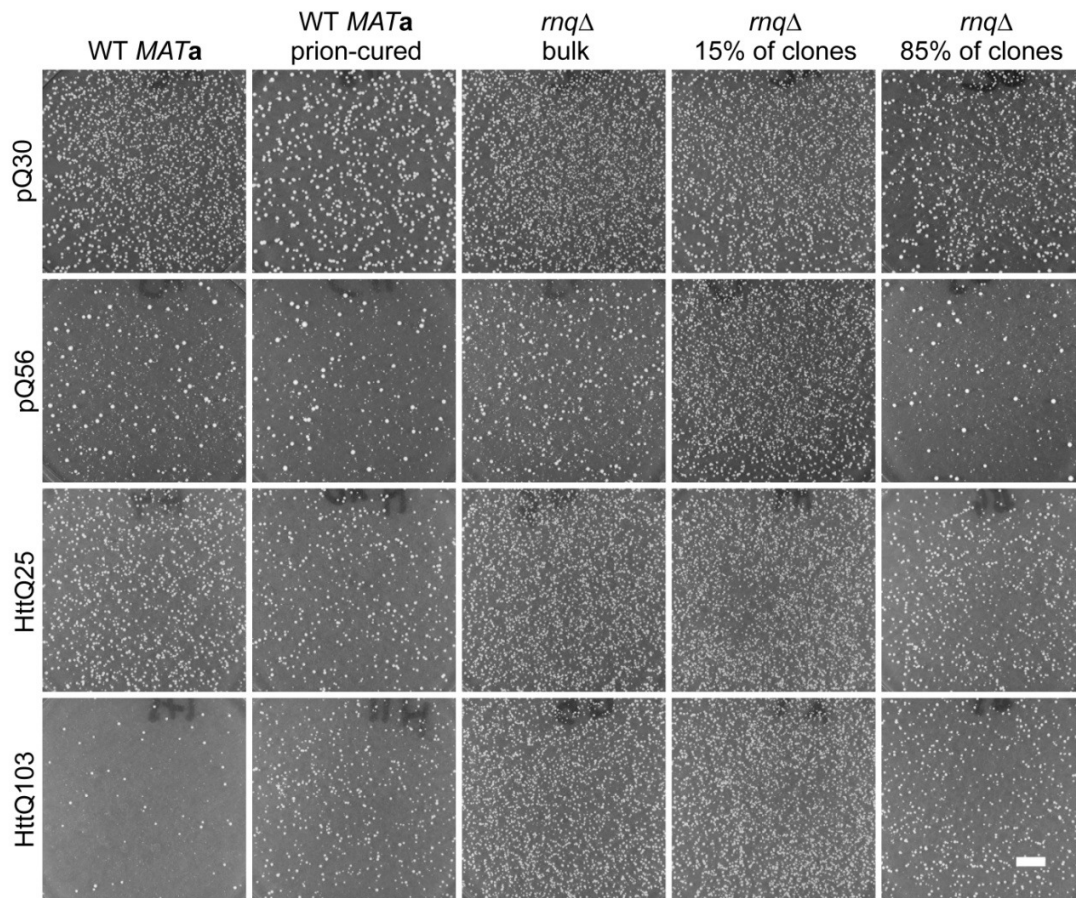
Supplementary Figure S6: Rescue strains and their phenotype for HttQ103. Identified strains were also examined regarding the cytostatic effect induced by HttQ103 expression (lower panel, left column). Some of the strains restore normal growth, while others rescue at least to some extent. Strong rescue is seen for *hsp104*Δ, *spt4*Δ, intermediate rescue for *scp160*Δ, and *pgd1*Δ while weak rescue is seen for *vps69*Δ. The images shown are representative results for these selected strains. *scp160*Δ exhibited generally less colonies in this experiment. The scale bar represents 10 mm.



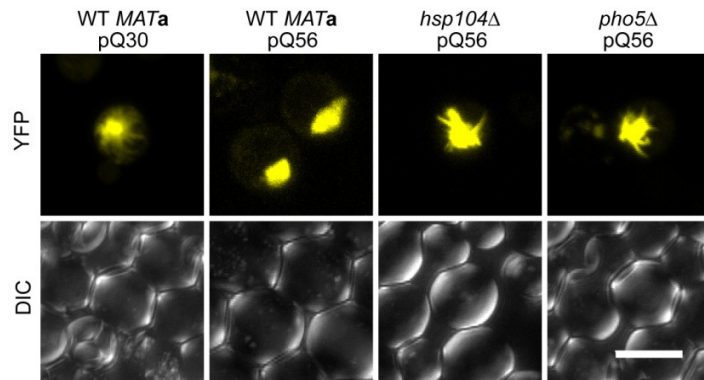
Supplementary Figure S7: Growth inhibition by HttQ103 is fully abolished in tetraploid yeast. (a) Toxicity of HttQ103 is evident in WT *MATa* cells. Slow colony growth is still observable under identical conditions in *MATa/a* (PY4995). Full rescue becomes evident for *MATa/a/a/a* (PY5006). **(b)** The same effect is observable in *MATα* strains, where *MATα/α* rescues partially and *MATα/α/α/α* rescues fully. The scale bars represent 10 mm.



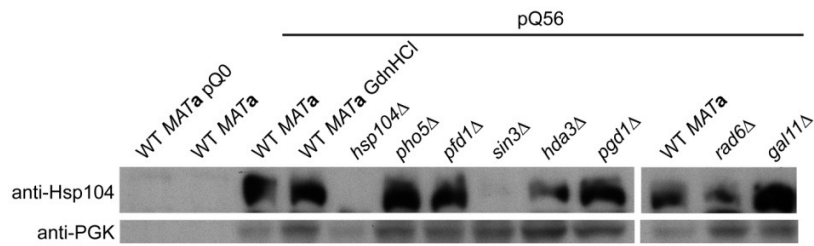
Supplementary Figure S8: GdnHCl reduces the *pica* phenotype of Q₅₆-YFP. (a) Addition of 4 mM GdnHCl to plates reduces the *pica* phenotype to undetectable levels (middle row versus upper row). The effect is similarly strong as the rescue effect of a *HSP104* deletion (lower row). The scale bar represents 10 mm. (b) FACS histogram of GdnHCl reduced pQ56 (red) compared to pQ0 (black) and pQ30 (blue). Only small differences are observed. (c) Even smaller differences between the three histograms are observed for *hsp104Δ*.



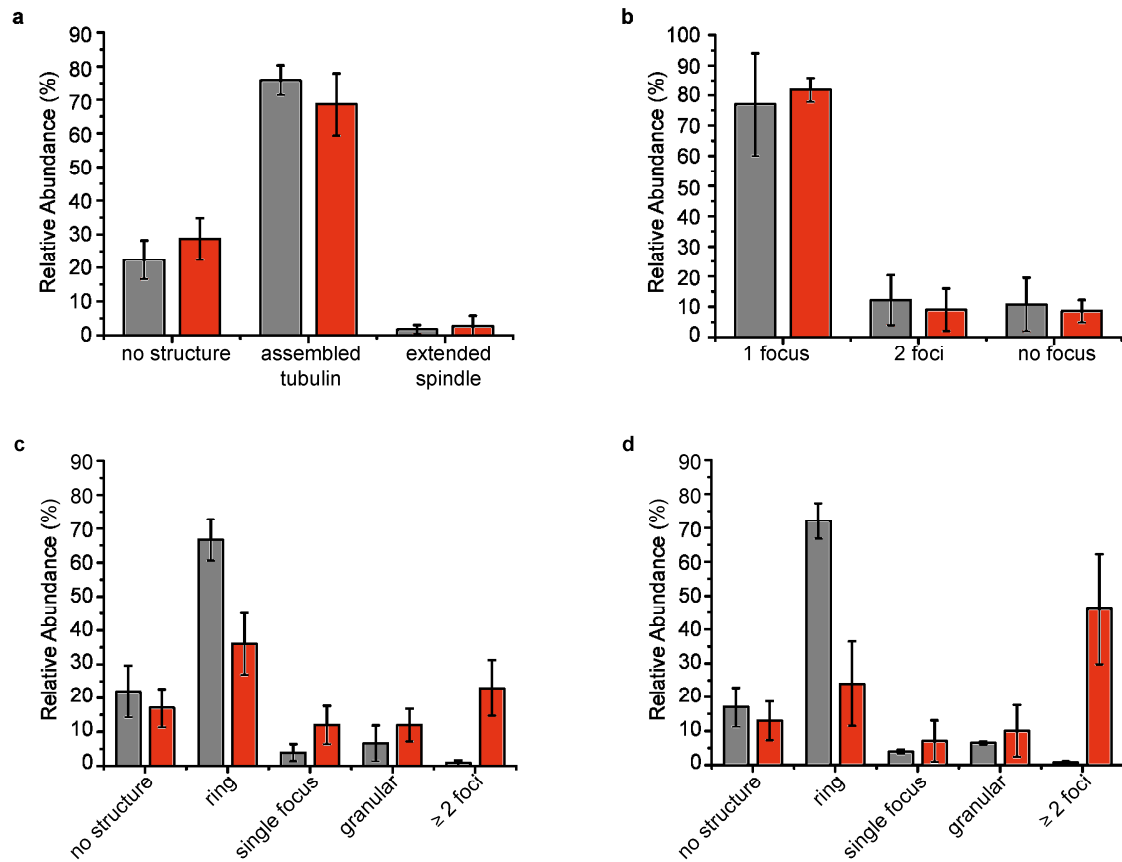
Supplementary Figure S9: The *pica* phenotype caused by pQ56 is independent of the prion state. Transformation assays comparing the reaction of the pQ30/pQ56 and HttQ25/HttQ103 systems in respect to endogenous prion phenotypes. The WT *MATa* strain BY4741 exhibits a growth inhibition phenotype for both systems. Curing the strain from prions by sequential passage on GdnHCl (prion-cured) abolishes the HttQ103 phenotype, while it is maintained for pQ56. Similarly, the transformation of bulk stock of an *RNQ1* deletion exhibits no phenotype for HttQ103 and a slight rescue effect for pQ56. This slight rescue is due to heterogeneity within the knockout strain, as clonally selected deletions for *RNQ1* abolish both phenotypes in 15% of transformed clones. In 85% however, *pica* through pQ56 is maintained, while it is lost for HttQ103. The scale bar applies to all photographs and represents 10 mm. All *rnq1Δ* clones ($n=15$) were sequenced to verify their genetic identity.



Supplementary Figure S10: The deletion of *HSP104* and *PHO5* alters aggregate morphology. Confocal microscopy of WT cells transformed with pQ30 reveals compact focal aggregation as well as fibrous protein deposits. This is in marked contrast to strongly fluorescent WT cells transformed with pQ56 which exhibit mainly compact aggregation. The deletion of *HSP104* as well as *PHO5* leads to a change in this aggregation pattern, rendering pQ56 transformants morphologically more similar to WT cells transformed with the pQ30 construct. All micrographs in the panel are maximum projections of image stacks recorded simultaneously in epifluorescence and DIC modes. The scale bar represents 5 μm for all micrographs.



Supplementary Figure S11: Hsp104 levels are unaltered for most group I strains. Western blotting against Hsp104 reveals that expression of Hsp104 is reduced in some of the knockout strains. While the level of Hsp104 is unchanged for most group I strains, the protein is properly absent in *hsp104*Δ. While *hda3*Δ and *rad6*Δ exhibit only slightly compromised Hsp104 levels, the protein is barely detectable in *sin3*Δ. The lysates of pQ0 and pQ30 transformed cells were diluted 15-fold to be in the dynamic range of immunogenic detection for the polyQ proteins in comparison to pQ56 transgenic cells.



Supplementary Figure S13: pQ56 interferes with septin assembly. Averaged morphological classification results for GFP-tagged reporter proteins transformed with the pQ0cherry construct (grey) and pQ56cherry (red) from three independent biological replicates are given. *n* is the cumulated number of cells evaluated. The error bars represent the standard deviation. (a) Results for Tub1-GFP (*n*=830 for pQ0cherry and *n*=742 for pQ56cherry). (b) Results for Nud1-GFP (*n*=748 for pQ0cherry and *n*=673 for pQ56cherry). (c) Results for Cdc10-GFP (*n*=967 for pQ0cherry and *n*=1436 for pQ56cherry). (d) Results for Shs1-GFP (*n*=1058 for pQ0cherry and *n*=1305 for pQ56cherry).

| Fluorescence Intensity | PolyQ Length | Ploidy State |
|------------------------|--------------|--------------------|
| very strong | Q8 | haploid |
| strong | Q20 | haploid |
| strong | Q16 | haploid |
| strong | Q12 | haploid |
| strong | Q20 | haploid |
| medium | Q30 | diploid and higher |
| medium | Q52 | diploid and higher |
| weak | Q52 | diploid and higher |
| weak | Q12 | diploid and higher |
| weak | Q28 | diploid |

Supplementary Table S1: Analysis of spontaneously occurring large colonies. Ten large colonies of different fluorescence properties from WT *MATa* plates transformed with pQ56 were picked and analyzed. The length of the polyQ stretch and ploidy was determined for each clone.

| Strain Number | Systematic Name | Standard Name |
|---------------|-----------------|-------------------|
| 589*** | YMR014W | <i>bud22Δ</i> |
| 1401*** | YIL009W | <i>faa3Δ</i> |
| 1440*** | YIL047C | <i>syg1Δ</i> |
| 1442** | YIL049W | <i>dfg10Δ</i> |
| 1484** | YIL093C | <i>rsm25Δ</i> |
| 1666** | YOR369C | <i>rps12Δ</i> |
| 2072 | YPL180W | <i>tco89Δ</i> |
| 2280** | YIL121W | <i>qdr2Δ</i> |
| 2293 | YIL134W | <i>flx1Δ</i> |
| 2316 | YIL157C | <i>coa1Δ</i> |
| 2345** | YIR009W | <i>msh1Δ</i> |
| 3223 | YBR085W | <i>aac3Δ</i> |
| 3765 | YDL068W | <i>YDL068WΔ</i> |
| 3770 | YDL073W | <i>YDL073WΔ</i> |
| 3923 | YDL225W | <i>shs1Δ</i> |
| 4278 | YDR442W | <i>YDR442WΔ</i> |
| 4296 | YDR462W | <i>mrp128Δ</i> |
| 4401 | YGL033W | <i>hop2Δ</i> |
| 5727 | YBR279W | <i>paf1Δ</i> |
| 6421* | YHR191C | <i>ctf8Δ</i> |
| 6422* | YHR193C | <i>egd2Δ</i> |
| 6423* | YLL030C | <i>rrt7Δ</i> |
| 6424* | YLL044W | <i>YLL044WΔ</i> |
| 6426* | YLL049W | <i>ldb18Δ</i> |
| 6797** | YJL029C | <i>vps53Δ</i> |
| 6861** | YJR063W | <i>rpa12Δ</i> |
| 6867 | YAL047C | <i>spc72Δ</i> |
| 7316*** | YNL138W | <i>srv2Δ</i> |
| 7395*** | YPL183W-A | <i>rtc6Δ</i> |
| 7533 | YKL096c-B | <i>YKL096c-BA</i> |

Supplementary Table S2: Growth restoring *MATa/a* strains uncovered in the library. 68 strains of the *MATa* library were identified to restore growth of Q₅₆-YFP expressing yeast. For all strains genomic DNA was purified and determined by PCR, whether they are in fact *MATa* or *MATa/a*. 30 strains were found to be true diploids heterozygous at the *MAT* locus. Many of those strains were already known to be *MATa/a* (*) or assigned with MET15 (***) or MET+ (***) in the library manual. For strain 7533 no conclusive result could be obtained.

| Gene Knockout | Strain Number | Gene function | Rescue Q ₅₆ -YFP | Rescue Htt103Q | Group |
|-----------------|---------------|---|-----------------------------|----------------|-------|
| <i>hsp104Δ</i> | 1514 | Protein folding | +++ | +++ | I |
| <i>pho5Δ</i> | 3232 | Phosphate regulation | +++ | +++ | |
| <i>pdf1Δ</i> | 1246 | Protein folding | +++ | ++ | |
| <i>hda3Δ</i> | 5594 | Chromatin organization, Transcription | +++ | o | |
| <i>cyk3Δ</i> | 3814 | Budding | + | +++ | |
| <i>gal11Δ</i> * | 1742 | RNA-Polymerase II regulation, subunit of Mediator Complex | +++ | ++ | |
| <i>sin3Δ</i> | 1695 | Chromatin organization | ++ | o | |
| <i>pgd1Δ</i> * | 4393 | RNA-Polymerase II regulation, subunit of Mediator Complex | +++ | ++ | |
| <i>rad6Δ</i> | 4425 | Protein degradation, Cell cycle control | ++ | +++ | |
| <i>bem2Δ</i> * | 7548 | Budding | +++ | + | II |
| <i>tif3Δ</i> | 5578 | Translation | +++ | o | |
| <i>asc1Δ</i> | 6556 | Translation | ++ | + | |
| <i>hof1Δ</i> * | 7817 | Budding | ++ | o | |
| <i>med2Δ</i> | 3701 | RNA-Polymerase II regulation, subunit of Mediator Complex | +++ | +++ | III |
| <i>sin4Δ</i> | 1976 | RNA-Polymerase II regulation, subunit of Mediator Complex | +++ | ++ | |
| <i>eap1Δ</i> | 7036 | Translation | +++ | o | |
| <i>ymr185wΔ</i> | 770 | Unknown | +++ | o | |
| <i>hsl7Δ</i> * | 3272 | Budding | +++ | +++ | |
| <i>cdc10Δ</i> | 3482 | Budding | +++ | o | |
| <i>swa2Δ</i> | 3679 | Budding / Vesicle transport COP | +++ | ++ | |
| <i>kre6Δ</i> | 5574 | Cell wall biogenesis | +++ | o | |
| <i>hnt3Δ</i> | 2514 | DNA repair | +++ | ++ | |
| <i>gpm2Δ</i> | 3717 | Metabolism | +++ | ++ | |
| <i>ldb16Δ</i> | 3413 | Mitochondrion | +++ | ++ | |
| <i>ybl094cΔ</i> | 3120 | Unknown | +++ | ++ | |
| <i>rox3Δ</i> | 3119 | RNA-Polymerase II regulation, subunit of Mediator Complex | ++ | ++ | |
| <i>spt4Δ</i> * | 6986 | RNA-Polymerase I/II regulation, pre-mRNA processing | +++ | +++ | |
| <i>scp160Δ</i> | 1343 | Translation | +++ | ++ | |
| <i>bfr1Δ</i> | 2454 | Translation, Nuclear segregation | +++ | ++ | |
| <i>vps69Δ</i> | 5504 | Vacuolar protein sorting | +++ | + | |
| <i>tho2Δ</i> | 2937 | Transcription | +++ | o | |
| <i>whi3Δ</i> | 2015 | Cell cycle control | ++ | ++ | |

Supplementary Table S3: Summary of the strains indentified in the genome-wide screen.

Gene function was assigned based on literature reviews. Most of the genes rescued to an extent that no growth difference was evident between cells producing Q₀-YFP, Q₃₀-YFP or Q₅₆-YFP, as indicated by +++ in the fourth column. Few strains rescued to a lesser extent (+ or ++). The same scale was applied for the rescue of HttQ103-GFP induced growth inhibition. If no rescue was detectable, this is indicated by an open circle. See Figs. S6 and S7 for representative images. Genes are classified according to FACS analyses, assigning them to the groups I, II or III. Transformation assays for each strain were performed at least in six separate replicates and

FACS measurements were four separate experiments for each strain (separate inoculum for every replicate). * *hsl7Δ*: two strains in the library (7539, 3272), of which both rescue; *gal11Δ*: two strains (1741, 1742) with similar results; *pgd1Δ*: two strains (4392, 4393) with similar results; *bem2Δ*: two strains (6152, 7548) with similar results; *hof1Δ*: two strains (7817, 608) with similar results; *spt4Δ*: two strains (4694, 6986) with similar results.